CONF-870812 - - 5

A review of the structural aspects of the Large Coil Task\*

M. S. Lubell, J. A. Clinard, J. W. Lue, J. N. Luton, T. J. McManamy, and S. S. Shen

Oak Ridge National Laboratory, Oak Ridge, Tennessee, U.S.A.

CONF-870812--8

DE87 007371

# 1 INTRODUCTION

The Large Coil Task (LCT) was initiated a decade ago by the United States (US), EURATOM (EU), Japan (JA), and Switzerland (CH) under the auspices of the International Energy Agency (IEA) to develop superconducting magnets for toroidal field coils for tokamak fusion reactors. Under the IEA agreement, EU, JA, and CH each fabricated one coil and shipped it to the Oak Ridge National Laboratory (ORNL), where the coils were assembled, along with three US coils (GD, GE, and WH), in the International Fusion Superconducting Magnet Test Facility (IFSMTF) which was designed and built at ORNL. The US Department of Energy is the operating agent.

The specifications were D-shaped coils with a bore of  $2.5 \times 3.5 \, m$ , a maximum field of 8 T, a weight of 45 tonnes or less, a current rating between 10 and 20 kA, stability in a background pulse field ramped repeatedly at 0.1 T/s to a peak of 0.2 T, recovery to the superconducting state when a full turn in the high-field region is driven normal, and the ability to withstand full out-of-plane loads induced when one neighbor is at full current and the other at zero current. internal design was left to each of the six teams and, as a result, there are significant differences among the coils, which were all fabricated by major industrial companies. Three of the coils (EU, CH, and WH) are cooled by force-flow (FF) supercritical helium at a pressure of 15 atm. The JA test coil and two of the US coils (GD and GE) have their conductors cooled by pool-boiling (PB) helium at atmospheric pressure. Five of the coils use niobium-titanium (NbTi) superconductor; one (WF) uses niobium-tin (Nb,Sn) conductor wound after reaction. Five of the coils are wound in pancakes; the GD coil is layer-wound. Five of the coils use austenitic stainless steel for the structural case; the WH structure is aluminum alloy plates with spiral grooves for the conductors. The EU stainless steel case is bolted, the GD case is welded and three cases are both bolted and welded.

In addition to the fact that six widely varying designs are being tested under similar conditions in the same test facility, the LCT project is unique in at least two other aspects. First, these are the

9th International Conference on Structural Mechanics in Reactor Technology

Lausanne, Switzerland - 17-21 August, 1987

<sup>\*</sup>Research sponsored by the Office of Fusion Energy. U.S. Department of Energy, under contract DE-ACOS-840R21400 with Martin Marietta Energy Systems, Inc.

## DISCLAIMER

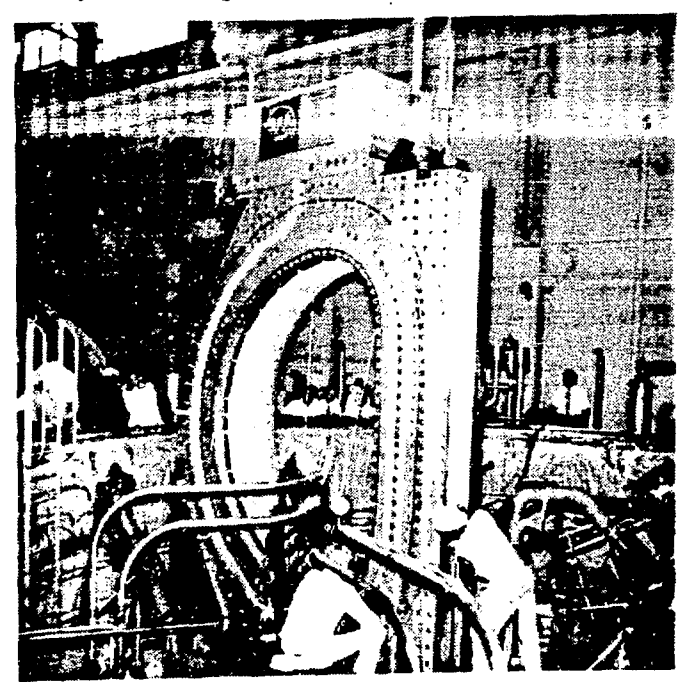
This report was prepared as an account of work sponsored by an agency of the United States Government. Neither the United States Government nor any agency thereof, nor any of their employees, makes any warranty, express or implied, or assu nes any legal liability or responsibility for the accuracy, completeness, or usefulness of any information, apparatus, product, or process disclosed, or represents that its use would not infringe privately owned rights. Reference herein to any specific commercial product, process, or service by trade name, trademark, manufacturer, or otherwise does not necessarily constitute or imply its endorsement, recommendation, or favoring by the United States Government or any agency thereof. The views and opinions of authors expressed herein do not necessarily state or reflect those of the United States Government or any agency thereof.

largest superconducting (SC) coils fabricated and tested to date for research and development of SC magnets. Second, as the magnets themselves are the experiment, they are each heavily instrumented; consequently, detailed information on thermal, electrical, and mechanical performance has been obtained, some for the first time on SC magnets of any size.

This paper concentrates on those aspects of the tests most relevant for fusion reactor magnets: the structural measurements and simulated nuclear heating tests. Other results have been recently reported (Lubell 1986, Shen 1986b). We use the data on the US PB coils (GD and GE) and the US FF coil (WH) to illustrate the results. It is gratifying to report that all six coils have achieved 100% design current at 8-T field and that in a symmetric torus arrangement all six coils have been simultaneously energized to 8 T.

#### 2 DESCRIPTION OF FACILITY

The test configuration chosen for the LCT is a torus of six coils, each with a 3.5- x 2.5-m D-shaped bore. Figure 1 shows the WH coil being put into the tank and illustrates the size of the facility. The coils are pushed together as closely as possible to decrease the number of ampere turns needed to reach the required 8 T at the winding where it cuts the equatorial plane. The coil bore is about half that being considered for reactors when the specifications were written, but the winding cross sections are full size. The design conditions are that when a single coil is at 100% current, the other five are at 80% current and the pulse coil is being repetitively pulsed to 0.2 T in "Extended cases" that the structure must withstand are one coil at 140% current with five coils at 100% and one coil at 110% with five coils at 90%, with the pulse field flattop at 0.28 T for both cases. In the design case the structural stress is limited to two-thirds yield, but in the extended cases 1.0 times yield is allowed if the low-cycle fatigue criteria are met.



The entire test stand. test coils, and pulse coils are enclosed in an 11-m vacuum vessel cryostat, The six test coils are attached through upper and lower collars to a hexagonal bucking post that supports them. The outer corners of the coils are clamped in torque rings at top and bottom. The bucking post has internal chambers filled with liquid helium (LHe) during operation, but the torque rings are

Fig. 1. WH coil being lowered into the IFSMTF vacuum tank.

cooled by conduction to the coils. The bucking post rests on a "spider frame," which in turn rests on rollers on pedestals cooled with liquid nitrogen (LN<sub>2</sub>) to intercept heat flowing up from the tank. Superconducting buses from each coil run through the vacuum tank wall to dewars where the transitions to room-temperature conductors are made. The "pulse coils" are mounted on a carriage on a circular track, with provisions for moving remotely to each test coil in turn. Nitrogen coolant for the copper conductors of the pulse coils is supplied through flexible stainless steel hoses. The carriage, track, The "cold wall," closely and pedestals are not actively cooled. enclosed by the vacuum vessel, consists of stainless steel panels supplied with LN2; their surfaces are covered with reflective blankets. The total cold mass is about 350 tonnes near LHe temperature and about 70 tonnes near LN2 temperature.

Vessel vacuum is provided by a system of mechanical, turbomolecular, and diffusion pumps. The tank is penetrated by 12 high-current leads, by numerous cryogenic helium and nitrogen lines, and by cables from more than a thousand sensors on the coils, test stand, and cold wall. Prior to cooldown, leakages into the tank are monitored by analyses of the tank atmosphere. When the test stand reaches operating temperature, cryopumping removes all but helium.

The facility refrigerator has a capacity of 1.5 kW at 4.2 K. During coil test operations it must simultaneously supply liquid at 4.2 K and atmospheric pressure to many components and helium at 3.8 K and supercritical pressure (15 atm) to the FF coils (Ryan 1979, Schwenterly 1986). During cooldown of the test array, the system must also provide circulation of helium at any desired temperature from 300 K to less than 10 K. Although the refrigeration system is marginal for such a large facility, with many "minor" modifications and careful attention to operating parameters and extraneous heat loads, it has proven adequate.

Cooldown is accomplished in three stages. At first, cooling is from  $\rm LN_2$  to the recirculating helium via heat exchangers. Near room temperature, the helium mass flow is only about 120 g/s at full compressor pressure, and  $\Delta T$  is set as high as the contraction stresses in the coils will allow. At about 100 K, cooling with  $\rm LN_2$  becomes relatively ineffective, and the refrigerator turboexpander is placed in service. During this stage, the cooldown rate is limited by the heat removal capability of the turbine. This in turn becomes ineffective at reduced temperatures, and at about 12 K the remaining heat is removed by LHe from 19,000-L and 2000-L storage dewars. Cooldown requires about four weeks.

## 3 TEST SEQUENCE

Testing began with single-coil tests of the JA and EU coils in their "domestic" facilities; continued in the IFSMTF with partial-array operation with the JA, GD, and CH coils when they were delivered to ORNL; and is now being completed in full six-coil operation. Fortunately, for a system so large and complicated, only one aborted cooldown and one successful cooldown were required for the partial array and for the full array. The first interruption was caused by contaminated welds in the GD coil, which leaked helium into the vacuum vessel when thermally strained by the initial stages of cooldown. The second was due to a leaking heat exchanger in the main cold box. The system has now been continuously cold since January 1986.

.

The rate of cooldown was limited by, among other things, the predicted abilities of the coils and test stand to bear the loads caused by nonuniform temperature distribution. The cooldown criteria adopted can be roughly summarized as: "Above 100 K, allow a temperature difference of no more than 50 K between inlet helium and any other spot; below 100 K, cool as rapidly as the refrigerator allows; keep the CH winding slightly warmer than its case." The last restriction was a caution to avoid breaking the epoxy bond between winding and case. No new leaks developed during the successful six-coil cooldown, and the area of a pre-existing small leak in a bus duct did not grow.

The coil tests were arranged in a sequence of increasing severity and have included steady and pulsed heat perturbation of coils at 100% of design value conditions for current, field, and pulse field. In order to ascertain the region in which a coil will operate stably, some of the tests ended in dumps. In these cases, the majority of the stored energy of the torus is dumped into an external dump resistor. A higher dump voltage gives a faster decay of the current, a lower hot-spot temperature in the coil, and lower strains; thus, there is a design trade-off to be made between voltage and temperature. The designers chose dump voltages of 2200-2500 V for the FF coils and 500-1000 V for the PB coils, whose insulation cannot be allowed to cover the conductor surface. Predicted hot-spot temperatures ranged from a low of 50 K to a high of 200 K.

#### 4 INSTRUMENTATION AND DIAGNOSTICS

There are more than 900 sensors for the test stand and refrigeration system. In addition, each coil has 200 to 300 diagnostic sensors measuring voltage, strain, temperature, magnetic field, changing magnetic field, flow pressure, acoustic emission, and displacements. In the bath-cooled coils many of the sensor leads penetrate the coil cases. The coils also contain heaters to permit stability and simulated nuclear heating tests. About 190 channels of experimental data are acquired through five front-end systems CAMAC-interfaced to a central processing computer (VAX 780), which in turn is connected to a cluster of computers for data storage and analysis (Baylor 1985).

Each coil has its own power supply (Wood 1985) capable of ±12 V and currents of 16 or 25 kA. The control system provides for synchronous, coordinated ramping up or down of the coil currents.

A unique quench detection system was designed and previously tested for the IFSMTF (Shen 1986a). The scheme was based on analog subtraction of self and neighboring pickup winding voltages from the coil voltage to yield a compensated signal proportional to a resistive (normal-zone) voltage. The compensated signals were input to quench detection modules that give a quench output signal to dump the coil if the signals exceed preset thresholds of voltage and duration.

## 5 FORCES

When tested by itself, the winding pack expands outward in the radial direction and compresses in the axial direction. Since these coils are D-shape, the deformation of the structure leads to a decrease of the vertical bore dimension and an increase in the horizontal bore dimension. This effect was measured and agrees well with calculation (Lue 1985, Luton 1984).

In the full-array tests, one coil at a time is the test coil and is charged to 100% current, while the other five are considered background coils and are charged to between 72% and 91% of design current. Different levels of current in the background coils are required to achieve 8 T in the test coil because of the different ampere-turns and winding pack dimensions of the coils.

The 8-T field occurs at the midplane at the inner bore of the straight leg of the D-shape. The maximum field of about 8.2 T is located toward the corner region. In the full-array (Standard-1) tests, the forces are primarily directed inward to the bucking post ranges from a low of 37 MN to a high of 54 MN per coil.

The steady-state out-of-plane load (also arising from the differences between the coils) ranges from zero to 10 MN. During a dump of the system, higher out-of-plane loads are experienced. For the structural cases used for the LCT coils, the Standard-1 out-of-plane loads are about one-third of the yield stress. The central forces to be experienced by machines now under design range from about 30 MN for TIBER II (Henning 1986) to 100 MN for a reactor. The out-of-plane forces should not be a problem for a reactor in which all coils are identical and will be energized and deenergized simultaneously. However, the overturning moments have always been a significant design problem for tokamak reactors. Even in this case, the new push to eliminate ohmic heating coils and go to dc tokamak operation will eliminate, to a large degree, the high overturning moments. the copper pulse coil creates a significant overturning moment on the test coils of about 5.8 MN-m (Mayhall 1987). This should be a sufficient demonstration to proceed with machines of the size of TIBER II.

# 6 STRUCTURAL CALCULATIONS

Structural calculations using the finite element method have been employed over a period of about ten years for the various phases of the LCT for: (1) confirming that individual coil stresses are within design allowables; (2) designing and validating the test facility and the pulse coil structural system; (3) interpreting and assessing measured data from the facility and coils; (4) aiding in selection of safe operating conditions during the remaining life of LCT; and (5) providing bases and tools for structural design analysis of future magnets.

In the early phase of structural design, ORNL performed preliminary six-coil analyses with simplified models of coils and facility; for each load case, the design teams were provided with the resulting sets of force and displacement boundary conditions. Each team then demonstrated compliance of its coil with the specified design criteria, though in several of the assessments for extended modes of operation the margin for compliance was slight and was achieved only after design modification. The individual coil finite element calculations performed by the various design teams were detailed and employed state-of-the-art techniques. For example, calculations for the WH coil were carried out using multilevel superelement models, allowing great detail to be considered.

During the period of coil fabrication and during early stages of coil delivery and installation, some facility redesign and modification were necessary. Realizing the potential importance of these variances, ORNL, starting some three years ago, undertook new six-coil finite

element calculations, which are now essentially complete. The present six-coil analysis strategy is based on the MSC/NASTRAN finite element program running on a CRAY computer. The three-dimensional model includes moderate detail of all significant structural components and contains some 21,000 elements. Extensive use of automated pre- and post-processors such as PATRAN and MOVIE.BYU allows visualization of computer input and output through color graphics. Decoupled magnetics programs are employed to generate the Lorentz force input. structural materials are assumed linear elastic. The coil winding is modeled as a solid orthotropic material and is based on the JA coil, The static (steady-state) analyses are carried out taking advantage of the six-part "near-geometric" symmetry and the various levels of loading symmetry afforded by the different six-coil tests. A multipass method is employed for rudimentary treatment of contact-gap boundaries occurring primarily at coil-to-facility interfaces.

Three sets of analyses have now been completed with the advanced models. We first solved for some 20 design and extended operational modes. Included in the cases without pulse coils were the Standard-1, the Alternate-C, the symmetric torus, the trio, and the Alternate-B cases. Some II design and extended cases with the pulse coils were considered, including modes of single pulse coil operation and mirror and cusp modes. These 20 solutions confirmed facility component structural integrity and adequacy of the design specifications for most operational modes.

The first set of calculations led to two additional sets of solutions, completing current studies. The initial Alternate-B solution signaled possible excessive out-of-plane motion of the toroidal field coil, jeopardizing the superconducting busses. The six-coil model was further modified to improve the nose-keyway region at the coil-to-bucking post interface, the reinforced regions of the torque ring system, and the collar-keeper slot regions. When Alternate-B was again solved, predicted motion could be marginally accommodated by the bellows system of the buses. We also re-solved four other cases with the "final" six-coil model: Standard-1, symmetric torus, single-coil at design current, and Standard-1 with the upper pulse coil at +4000 A. These solutions should afford interesting comparisons among predicted and measured mechanical responses and are expected to be included in later, more detailed papers

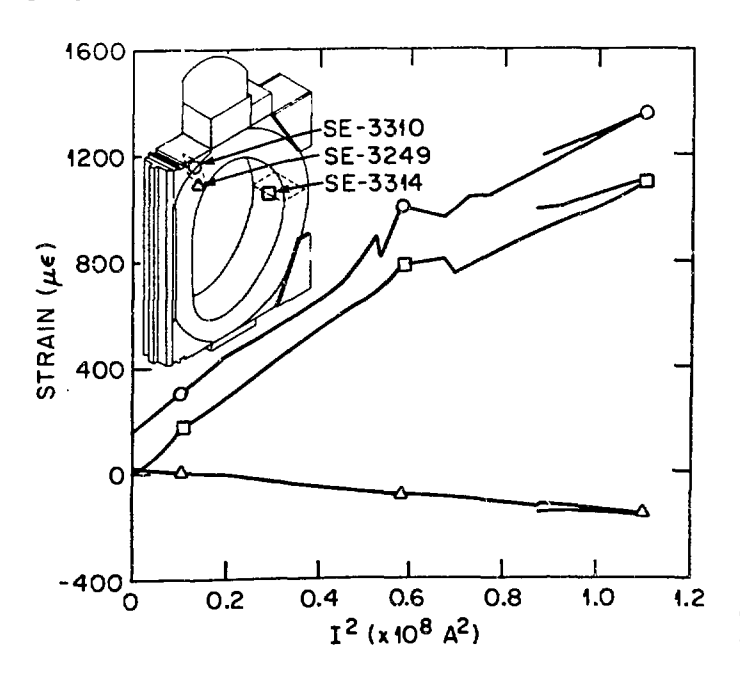
The final set of calculations isolates the bolting systems of the pulse coils and their supports. These fasteners must sustain the cyclic loading produced by pulse coil operation, avoiding fatigue failure. Auxiliary models are required to produce the necessary detail at the bolting level and to eliminate unneeded detail for facility components and TF coils, while retaining only gross structural mechanisms for transmitting Lorentz forces. Included in the details of the auxiliary pulse coil model are the individual bolts, modeled as beam elements with axial preload captured as superimposed thermal Mechanisms for gap formation, friction, and slippage (when loads. bolts are in slots) are also included. Cases for the +2000 A mirror and the upper pulse coil at +4000 A were solved and indicate that the design-life cycles are acceptable, if, as shown by bench tests, the cast epoxy shims do not disbond during cooldown and so can absorb some shear load.

# 7.1 GE coil

The GE coil is constructed of conductors with semi-monolithic NbTi subelements cabled around a copper core. The conductor is sized into three grades with the overall width fixed at 4.18 cm and the thickness varied from 0.75 to 1.03 cm. It is flat-wound in pancakes (with 12 active pies and two dummy pies) without interpancake cross-cooling channels. The winding pack is enclosed by 5-cm-thick structural plates of AISI 316LN stainless steel, which also serves as its helium bath container. Specially machined G-10 fillers were made to achieve good fitting between the winding and the case. The plates are bolted and welded to make the case helium tight.

Displacements of the coil winding relative to the case during current charges were measured by Moving Slug Displacement Transducers (MSDTs) (similar to the MEDTs of Ellis, 1978). The measured displacements from side plates were about 0.8 mm at 100% design current in both single-coil and full-array operation. The winding had a radial displacement from the inner case ring of about 3.2 mm in single-coil charge and 2.7 mm in full-array charge. The conductor configuration and the interturn insulation made the coil rather spongy radially.

Scores of strain gauges are attached to the conductor and coil case to monitor the winding and structural strains during current charges. Figure 2 shows the strain behavior of some representative gauges during a single-coil charge. All strains are more or less proportional to the square of the current as was expected. Strains as high as 1200  $\mu\epsilon$  and 1680  $\mu\epsilon$  on the conductor were observed in single-coil (6-T field) and full-array charges, respectively. The strains on the coil case reached only 180  $\mu\epsilon$  in single-coil charge and 900  $\mu\epsilon$  in full-array charge. This large disparity obtained in the strain measurements on the winding and the case indicates that the strain on the winding did not transfer well to the case. The mechanical coupling between them seems rather poor. Also, the strains on a few conductor subelements showed sudden jumps at some currents, and this type of behavior was repeated at



different charges. This may indicate that some of the subelements soldered to the conductor core are disbonded.

In the full-array charge, the coil received a centering force of about 39 MN and an out-of-plane load of about 1 MN. Rowever, during a full-array dump with the GE coil as the test coil, it experienced an out-of-plane load of up to 11.2 MN some 20 s after

Fig. 2. GE representative strains, winding and case, single-coil operation.

after the dump was initiated. This was caused by the different decay time constants of the six coils.

Acoustic emissions of the coil during current charge were monitored by sensors mounted on the surface of the coil case. Qualitative observation of the signals showed few acoustic emissions below about 60% of the design current. The frequency and size of the events then increased steadily toward higher current. They subsided significantly during ramp-down and in subsequent runs. Coincidences between the acoustic emissions and compensated coil voltages were rare.

#### 7.2 GD coil

The GD coil (Haubenreich 1982) is constructed of conductors with a compact monolithic structure, consisting of a Rutherford-style NbTi superconducting cable soldered into the slot of a rectangular copper stabilizer. Side fins are machined along the stabilizer to provide extra cooling surface and to increase the local LHe inventory. The conductor is graded into 3 sizes and edge-wound into 14 layers. Interturn and interlayer insulation directs helium bubbles in a way that minimizes vapor accumulation. This coil has previously been cooled down and electrically tested in the partial-array test (Haubenreich 1986).

The GD coil was tested to full design current of 10.2 kA as the test coil in full-array mode. The maximum field was about 8.2 T in the corner region.

In single-coil stability tests, unconditional recovery of a whole turn driven normal was observed up to 100% design current. However, the slow recovery rate indicated a continuing heat input from the Kapton-covered heater wire, or a substantial degradation of heat transfer to helium, or both. In full-array tests at 100% current, cold-end recovery was observed, in contrast to the predicted unconditional recovery. Copious vapor accumulation due to the large heating power required to create a normal zone was thought to cause this degradation.

Mechanical behavior of this coil was monitored by strain gauges on conductor and structural case, winding displacement transducers, and acoustic emission (AE) sensors on coil case. As with the other two PB coils, the measured strains on the conductor are much higher than those on the case, and the former are higher than predicted while the latter are lower. The displacement of the winding from the case is substantial under loads, and the correlation of AE signals to the compensated coil voltage spikes is poor. These all pointed to the fact that the mechanical coupling between the winding and the case is probably rather poor.

# 7.3 WH coil

The WH coil uses a Nb<sub>3</sub>Sn cable-in-conduit superconductor cooled by 4 K, 15-atm, FF supercritical helium. The conductor is formed from 486 strands which are fully transposed, each strand having 2869 3.5- $\mu$ -diam niobium filaments imbedded in a 0.43-mm-diam bronze core. The core is sheathed with copper, and the final configuration is 63% copper and 37% bronze, niobium, and Nb<sub>3</sub>Sn. The cabled strands are sheathed with a jacket of JBK-75, a modified version of the superalloy A286. This material was chosen for its strength and its ability to tolerate the 15-h, 700°C heat treatment used to react the Nb<sub>3</sub>Sn. Considerable

effort was expended to produce a leak-tight and defect-free weld in the sheath. Eddy current inspection techniques were developed to detect flaws larger than allowed by fracture mechanics considerations (0.44 mm) (Kibbe 1985).

The reacted superconductor was wound four-in-hand into a set of aluminum plates with machined grooves, and the 24 supporting plates were bolted together to form the coil. One effect of this distributed structure was to lower the average current density in the winding pack. As a result, in order to make a peak field of 8 I on the horizontal midplane, the WH coil required approximately 20% more ampere-turns than the average of the other five LCT coils. The plates were all split to reduce eddy currents during charge and discharge. However, the plates appear to have been shorted together during fabrication; consequently, during a dump over 20% of the stored energy is dissipated in the plate structure through the mutual coupling (Luton 1986).

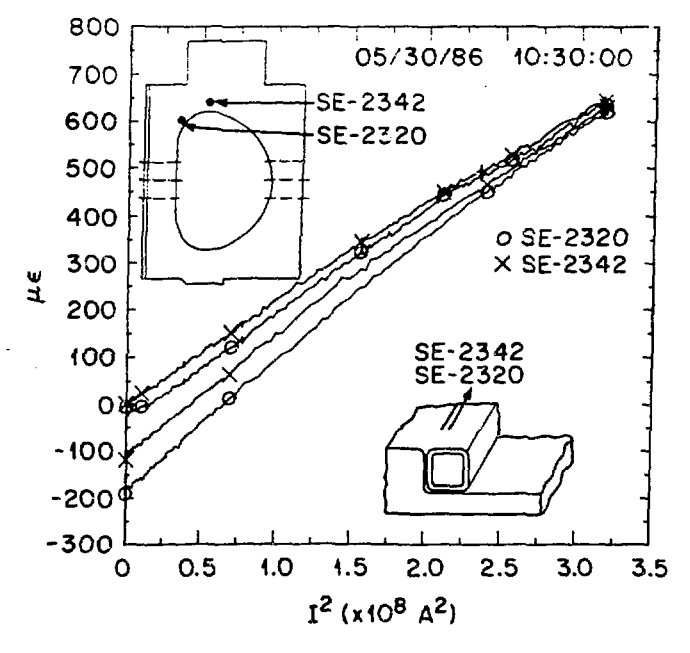
The net centering force load on the WH coil during the Standard-I test was 54 MN. The out-of-plane load during this test was 0.8 MN. A six-coil dump occurred during the GE Standard-I test, and during this discharge the WH coil out-of-plane load peaked at 7.5 MN.

Strain gauge data were recorded from 27 gauges mounted on the aluminum structure and 15 gauges on the conductor sheath. In general, the measured strains on both the conductor and structure were low and proportional to the square of the current even at low current levels. This indicates that the loads are effectively coupled into the distributed structure. The largest strains observed in the aluminum structure were 1000  $\mu\epsilon$  during the single-coil test and 1240  $\mu\epsilon$  during the Standard-1 test. The peak conductor strains were 650  $\mu\epsilon$  for the single-coil and 800  $\mu\epsilon$  for the Standard-1 test. Figure 3 shows the highest conductor strains vs I² for the single-coil test.

Unlike the PB coils, a correspondence was observed between the occurrence of compensated voltage spikes and bursts of acoustic emission, indicating a good contact between conductor and structure.

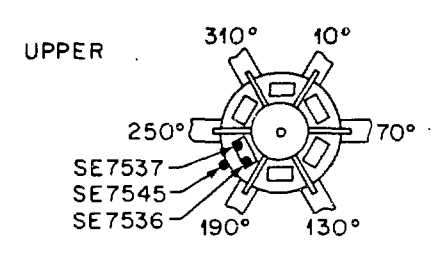
# 8 FACILITY STRAINS

Three hundred facility strain gauge channels were monitored during the



testing. The single-coil and Standard-1 test series were not expected to produce large stresses in the facility, and in general the measured strains were low. highest facility strains occurred during single-coil testing the region of the support collar corners. Figure 4 shows the location of strain gauges oπ the support collars at each

Fig. 3. Peak strains, with hysteresis, for WH conductor in single-coil operation.



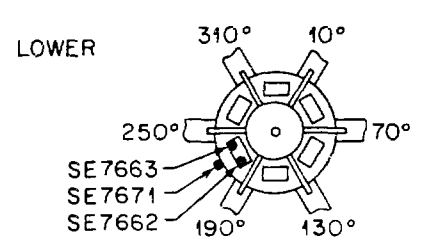


Fig. 4. Strain gauge locations on the GD sector of the support collars.

end of the bucking post. coil is held to the post by a through the support wedge collar. In a single-coil test, as the coil tries to go around, it pushes inward on the bucking post and outward on the support In the Standard-1 tests. the large centering forces reduce substantially the net outward load on the support Figure 5 shows this collar. effect for the GD coil. largest strain measured  $1600~\mu\epsilon$  in the support collar corner for the WH single-coil test. In the Standard-1 test

for the WH coil and in the symmetric-torus test, all the coils reached 8 T, but the highest facility strain recorded was only 600  $\mu\epsilon$ .

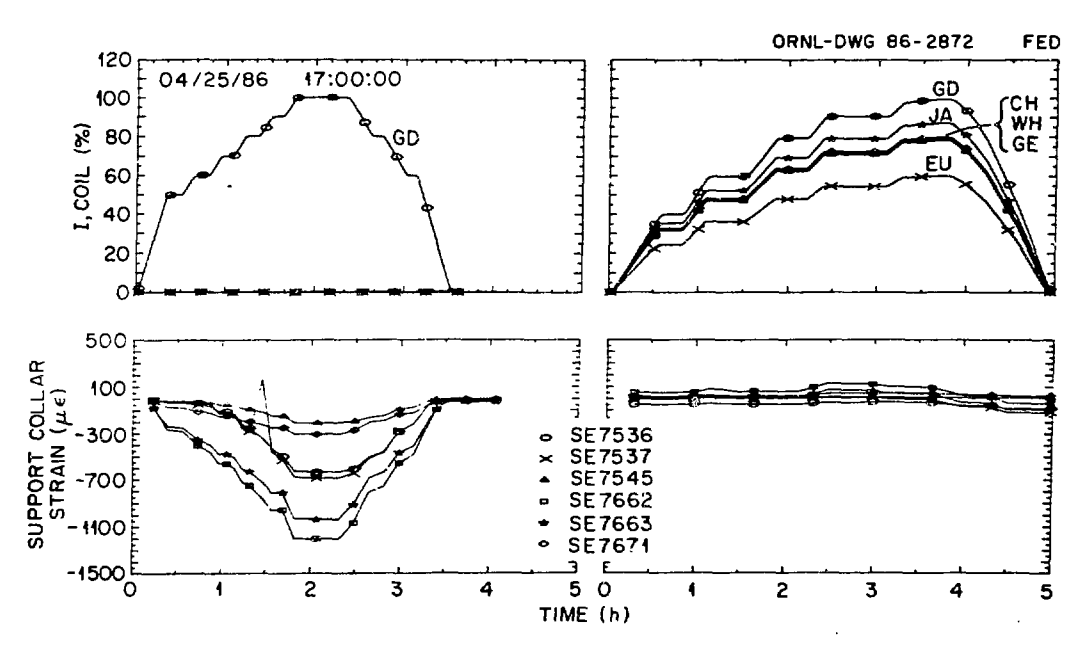


Fig. 5. Coil currents and collar strains for (a) GD alone and (b) six-coil test.

## 9 SIMULATED NUCLEAR HEATING

All fusion reactors will produce significant nuclear heating. The actual amount impinging on the SC magnets is strongly dependent on machine design. Since this amount is unknown for SC magnets, the recent design studies for TFCX (TFCX Preconceptual Design Review 1984) and the EPR assumed nuclear heating rates of 10 mW/cm³ for the nominal

design and 50 mW/cm³ for a high-performance (optimistic) design. It is expected that this power density would not exist over the whole volume but would attenuate rapidly with depth. For the FER project in Japan, a peak value of 1 mW/cm³ has been assumed (Iida 1986). The Next European Torus (NET) design used FF cooling for the coils and expected an average nuclear heating density of  $0.058 \text{ mW/cm}^3$  over the whole winding volume.

Simulated nuclear heating tests were performed on all three PB coils and one FF coil (the CH coil). The PB coils were tested by simultaneously powering all the available heaters in the coil for 60 s. The heating time was chosen to get a steady-state environment yet not create too much pressure rise in the coil and heat load to the refrigerator. Local unit power densities of up to 50 to 70 mW/cm³ were used. The test was performed up to 100% design current in both the single-coil and full-array test. All three coils passed these tests with no normal zone or thermal runaway induced.

For the CH coil, the heat was generated by constant ohmic heating applied to 11 full-turn heaters while the coil was ramped up to its nominal current. The heat input to the winding was also measured by the heat loss of the winding. The total heating power was approximately 260 W, corresponding to a mean power density of  $3.6~\mathrm{mW/cm^3}$  in the heated volume. Using the volume of the CH coil winding (2.13 m³), an average power density of  $0.12~\mathrm{mW/cm^3}$  is calculated. This power density is twice as large as the value specified for the TF coils of the NET design.

## 10 CONCLUSION

All six LCT coils were energized to full design current and field without any problems such as training. These are the largest coils ever to produce an 8-T field. In the symmetric torus arrangement the currents were suitably adjusted so that all the coils were energized simultaneously to an 8-T field, giving a total stored energy of 760 MJ.

Heat perturbation experiments were successfully performed on the three US coils. Recovery to the superconducting state from a whole turn driven normal was demonstrated at 100% design current in an 8-T field. The FF WH coil had a very high stability margin (>10³ mJ/cm³) even though the thermal margin to the current-sharing state was small. Although the PB coils were cryostable, there was some indication that vapor accumulation degraded the heat transfer. Nevertheless, this should not detract from the highly successful demonstration of simulated nuclear heating, which provides confidence that the design values used in reactor studies can most likely be achieved.

A comparison of the strains on the conductor and case of the PB coils, along with analysis of the displacements and acoustic emission, leads to the conclusion that the mechanical coupling between the winding and the structural case is poor. The FF coil which has its conductor restrained in grooves had good coupling.

The central forces, which spanned the range from a low of 37 MN to a high of 54 MN (for the WH coil), apparently have created no problem for any of the structures. So far the out-of-plane forces have been deliberately limited to about one-third of yield stress, but they will be increased in the extended phase of the test program later this year.

With more than half of the planned LCT experimental program completed, the assurance that large SC magnets can be developed for fusion reactors already has been greatly enhanced.

This work has been performed in the framework of the IEA-IMPLEMENTING AGREEMENT FOR A PROGRAMME OF RESEARCH AND DEVELOPMENT ON SUPERCONDUCTING MAGNETS FOR FUSION POWER, ANNEX I, "LARGE COIL TASK," between US/DOE, EURATOM, Japan, and Switzerland. Thus, the reported results could only be achieved by the common effort of all participants involved. The dedication and skill of the operators of the test facility at ORNL, under the direction of W. A. Fietz, are gratefully acknowledged.

#### REFERENCES

- Baylor, L. R. et al. 1985. Implementation and operation of a VAX-based data acquisition system for the Large Coil Program. Proc. 11th Symp. on Fusion Engineering, Vol. 1:605-608. IEEE: New York.
- Ellis, J. F. & P. L. Walstrom 1978. A moving coil linear variable differential transformer. Rev. Sci. Instr. 49:398-400.
- Haubenreich, P. N. et al. 1982. Superconducting Magnet Development Program. Nucl. Fusion 22:1209-1236.
- Haubenreich, P. N. 1986. The Large Coil Task and results of testing U.S. coils. Presented at the Applied Superconductivity Conference, Baltimore, MD, Sept 28-Oct 3.
- Henning, C. D. & B. G. Logan (eds.) 1986. TIBER II. UCID-20863. Lawrence Livermore National Laboratory.
- Iida, F. (JAERI). 1986. Private communication.
- Kibbe, R. K. et al. 1985. Experience highlights from the design and manufacture of U.S. LCT coils. IEEE Trans. Magn. MAG-21:234-237.
- Lubell, M. S. et al. 1986. The international Large Coil Task: testing of the largest superconducting toroidal magnet system. Presented at the 11th International Conference on Plasma Physics and Controlled Nuclear Fusion Research, Kyoto, Japan, Nov. 13-20.
- Lue, J. W. et al. 1985. Partial-array test results in IFSMTF. Fusion Technol. 8(2):807.
- Luton, J. N. et al. 1984. Preliminary results of the partial-array LCT coil tests. IEEE Trans. Magn. MAG-20:238-241.
- Luton, J. N. et al. 1986. A study of eddy-current effects in the structure of the Westinghouse LCT coil. Presented at the Applied Superconductivity Conference, Baltimore, MD, Sept 28-Oct 3.
- Mayhall, J. A. 1987. Private communication.
- Ryan, T. L. & R. E. Stamps 1979. The liquid helium system for the Large Coil Test Facility. Proc. 8th Symp. on Engineering Problems of Fusion Research, p. 1187.
- Schwenterly, S. W. et al. 1986. Performance of the IFSMTF helium refrigerator in Partial-Array Tests. Adv. Cryog. Engr. 31:617-626.
- Shen, S. S. et al. 1986a. Proc. 9th Int. Conf. Magnet Technology, p. 811.
- Shen, S. S. et al. 1986b. First results of the full-array LCT coil tests. Presented at the Applied Superconductivity Conference, Baltimore, MD, Sept 28-Oct 3, 1986.
- TFCX Pre-conceptual Design Review 1984. Princeton: Princeton Plasma Physics Laboratory.
- Wood, R. J. et al. 1985. Problems and solutions of the IFSMTF power and switch system. Proc. 11th Symp. Fusion Engineering, Vol. 1:692-695.